frontiers | Frontiers in Soft Matter

TYPE Mini Review
PUBLISHED 01 June 2023
DOI 10.3389/frsfm.2023.1193904

OPEN ACCESS

EDITED BY
Yanlei Yu,
Fudan University, China

REVIEWED BY
Ingo Dierking,
The University of Manchester,
United Kingdom

*CORRESPONDENCE
Aleksander Zidanšek,
aleksander.zidansek@ijs.si

RECEIVED 25 March 2023
ACCEPTED 10 May 2023
PUBLISHED 01 June 2023

CITATION
Hölbl A, Ranjkesh A, Abina A, Kralj S and Zidanšek A (2023), Phase behavior of nematic-nanoparticle mixtures. *Front. Soft. Matter* 3:1193904. doi: 10.3389/frsfm.2023.1193904

Phase behavior of nematic-nanoparticle mixtures

Arbresha Hölbl[1], Amid Ranjkesh[2], Andreja Abina[3], Samo Kralj[1,2] and Aleksander Zidanšek[1,2,3]*

[1]Faculty of Natural Sciences and Mathematics, University of Maribor, Maribor, Slovenia, [2]Condensed Matter Department, J. Stefan Institute, Ljubljana, Slovenia, [3]Jožef Stefan International Postgraduate School, Ljubljana, Slovenia

We study the effects of nanoparticles (NPs) on thermotropic nematic liquid crystals (LCs) in relatively dilute NP–LC mixtures. We are interested in the fundamental generic mechanisms that quantitatively and qualitatively affect the phase behavior of LCs. A simple molecular field analysis shows that a phase transition will likely occur upon entry into the ordered phase. Moreover, the interaction between nematogenic NPs and LCs could force a sergeant–soldier-like behavior, in which only the phase behavior of one component is affected despite the symmetric appearance of the coupling term. When NPs are anisotropic, their influence on LC phase behavior can be qualitatively different depending on the anchoring, even in the absence of the disorder. We illustrate numerically that a random-field-type disorder might impose either short-range, quasi-long-range, or even long-range order, which might survive.

KEYWORDS

nanoparticles, phase behavior, surface interactions, disorder, sergeant–soldier behavior

1 Introduction

Mixing soft materials with appropriate nanoparticles (NPs) can yield effective materials exhibiting new or anomalously enhanced properties (Balazs et al., 1979; Hamley, 2003). If soft materials exhibit a kind of orientational or translational order, the richness of the resulting qualitatively different effective materials explodes. Liquid crystalline (LC) materials are an excellent example. They combine a unique combination of liquid character, order, softness, and optical transparency (de Gennes, 1995; Kleman and Lavrentovich, 2003; Oswald and Pieranski, 2019). The liquid character enables relatively simple preparation of mixtures. Order in LC matrices can give rise to long-range forces among immersed NPs (Poulin et al., 1979; Pires et al., 2007). Softness can enable relatively strong responses in the LC matrix in the presence of adequate NPs (Lelidis et al., 1993; Li et al., 2006; Palffy-Muhoray, 2007). Furthermore, optical transparency enables relatively simple observation of NP-driven changes (Poulin et al., 1979; Pires et al., 2007). It should be noted that long-range forces among NPs could trigger the self-assembling of NPs, which can open different structural pathways (Hegmann et al., 2007; Bisoyi and Kumar, 2011; Lagerwall and Scalia, 2012; Lagerwall and Scalia, 2017).

Nematic (de Gennes, 1995; Kleman and Lavrentovich, 2003; Oswald and Pieranski, 2019) orientational order represents the simplest LC phase structure. It is described by the nematic molecular field. In bulk nematic equilibrium, the molecular field is uniaxial and spatially homogeneously aligned along a single symmetry-breaking orientation. Local uniaxial order is commonly described in terms of the nematic director field $\vec{n}$ and the nematic order parameter S. The unit vector points along the local uniaxial direction, where the states $\pm\vec{n}$ are physically equivalent. The amplitude field S describes the amount of

ordering along $\vec{n}$. In thermotropic LCs, one commonly obtains a nematic phase by cooling it from the isotropic (ordinary liquid) phase in which $S = 0$. Perturbed nematic order could generally exhibit biaxial states, which requires description in terms of the tensor nematic order parameter Q (see Supplementary Appendix SA).

Appropriate NPs could influence the nematic order via different generic mechanisms if inserted into nematic LCs. Important controlling parameters are the concentration of NPs, geometrical shape (Bellini et al., 2000; Kyrou et al., 2018; Kyrou et al., 2020; Skarabot et al., 2022), NP surface treatment (Nobili and Durand, 1992; Lavric et al., 2013a; Oswald and Pieranski, 2019; Kyrou et al., 2020), material characteristics of NPs (Mertelj et al., 2013; Kumar, 2014; Moghadas et al., 2015; Poursamad and Hallaji, 2017; Emdadi et al., 2018a; Emdadi et al., 2018b; Drozd-Rzoska et al., 2019; Jahanbakhsh et al., 2019; Poursamad and Emdadi, 2019; Lahiri et al., 2020; Bury et al., 2022; Ma et al., 2022; Sumandra et al., 2022), and LC material properties (de Gennes, 1995; Kleman and Lavrentovich, 2003; Oswald and Pieranski, 2019). Furthermore, NPs could effectively impose qualitatively different disorders on the LC order (Harris et al., 1973; Cleaver et al., 1996; Crawford and Žumer, 1996; Radzihovsky and Toner, 1997; Popa-Nita and Kralj, 2006). Most studies focusing on the impact of the disorder are performed in LC-aerosil mixtures, which can exhibit at least three qualitatively different disorder characteristics (Jin and Finotello, 2001; Bellini et al., 2002; Leon et al., 2004; Rotunno et al., 2005; Buscaglia et al., 2006; Cordoyiannis et al., 2006; Relaix et al., 2011). Furthermore, NPs could enforce LC matrix topological defects (TDs) (Mermin, 1979; Kurik and Lavrentovich, 1988) in the nematic orientational order. TDs correspond to topologically protected, elastically distorted regions in the orientational order. Nematic LCs could host either point or line defects (Schopohl and Sluckin, 1987; Kurik and Lavrentovich, 1988; Lavrentovich, 1998; Kralj and Virga, 2001). Generally, TDs can strongly interact with NPs, opening the door to predetermined and controlled superstructures stabilized by TD–NP interactions (Kikuchi et al., 2002; Yoshida et al., 2009; Karatairi et al., 2010; Liu et al., 2010; Rozic et al., 2011; Coursault et al., 2012; Wang et al., 2012; Lavric et al., 2013a; Lavric et al., 2013b; Liu et al., 2018).

This paper considers different NP-driven generic mechanisms via which NPs impact nematic thermotropic behavior.

2 Results

Mixtures of nematic LCs and NPs can exhibit complex configurations. In the following, we present some qualitatively different scenarios and discuss generic mechanisms.

Supplementary Appendix SB illustrates a simple mean-field Maier–Saupe analysis that reveals the type of coupling terms in a mixture of two nematic mesogens. It yields the following free energy density expression:

$$f \approx f_0 + (1-p)\left(a_0\left(T-(1-p)T^*\right)S^2 - bS^3 + cS^4\right), \\ +p\left(A_0\left(T-pT_2^*\right)S_2^2 - BS_2^3 + CS_2^4\right) - wSS_2. \quad (1)$$

Here, $S \equiv S_1$ and S_2 label the nematic order parameters of the first and second components. Their volume concentrations are given by $p_1 = 1 - p$ and $p_2 = p$, respectively. Quantities a_0, b, c, $T^* \equiv T_1^*$, A_0, B, C, and T_2^* are material constants, in which we neglect temperature dependencies in the temperature windows of our interest. Furthermore, f_0 determines the contributions of the remaining degrees of freedom.

FIGURE 1
Typical phase separation pattern on entering the nematic LC phase in a nematic-NP mixture. In the case shown, NPs are spherical. Regions are exhibiting i) relatively strong nematic and ii) essentially isotropic (or paranematic) order, which are i) poor and ii) rich in NP content, respectively.

Let us suppose that the first and second components represent LC molecules and NPs, respectively, and the volume concentration of NPs is given by $p \equiv p_2$. The presence of NPs introduces an additional contribution equal to $p(1-p)a_0T^*S^2$ in the LC condensation term in Eq. 1.

This term resembles the structure of the so-called Flory–Huggins free energy contribution (Onsager, 1949; Flory, 1956; Doi, 1981):

$$f_{FH} = p(1-p)\chi, \quad (2)$$

where χ stands for the Flory–Huggins constant. For a positive value of χ, this term enforces phase separation if χ exceeds the critical value χ_c. Suppose that in the absence of ordering, it holds $\chi^{(I)} < \chi_c$, where $\chi^{(I)}$ denotes the Flory–Huggins constant in the isotropic phase (where $S = 0$). On entering the nematic phase, the effective Flory–Huggins interaction increases:

$$\chi^{(N)} = \chi^{(I)} + a_0T^*S^2. \quad (3)$$

In most LCs, the second term, "switched-on" in the nematic, is relatively strong. Consequently, on cooling an isotropic mixture to the nematic phase, phase separation is generally likely to occur (Anderson et al., 2001). Figure 1 illustrates a typical phase separation in a mixture of nematic and spherical NPs (i.e., $S_2 = 0$) on entering the nematic phase. In the phase separation regime, the regions exhibiting essentially strong and low nematic LC order coexist.

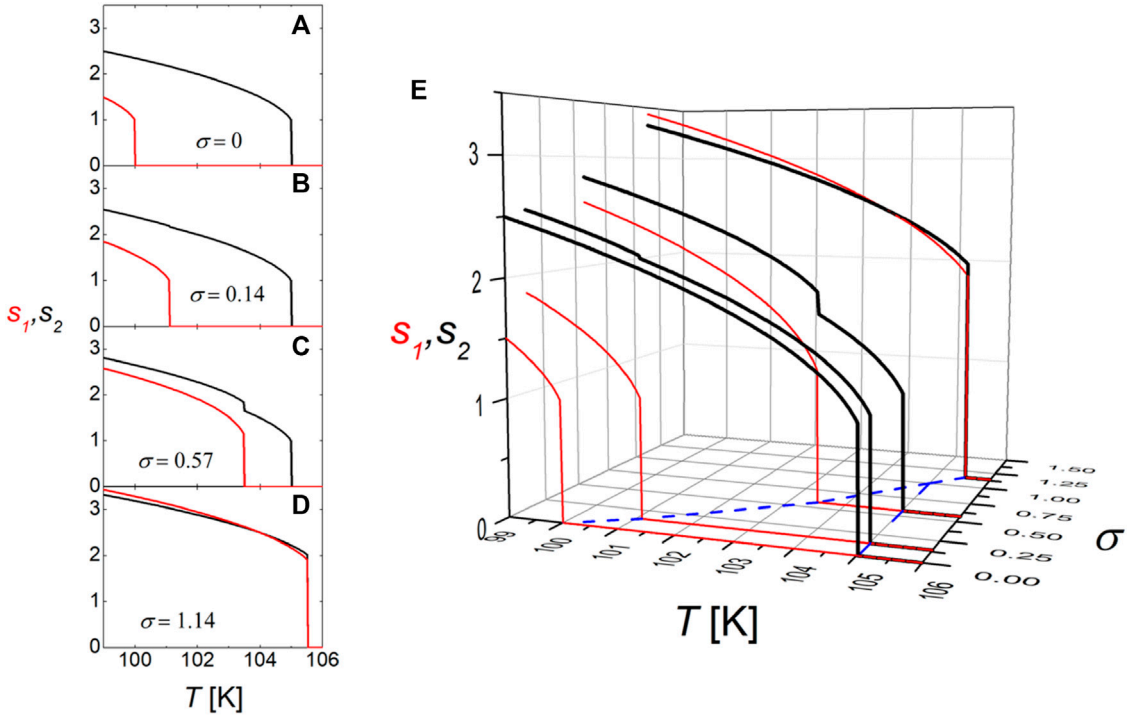

FIGURE 2
"Sergeant–soldier" behavior. For the dimensionless coupling strength $\sigma = w/w_c$, below the critical value (corresponding to w_c), on increasing σ, the phase transition temperature of "soldier" (S_1) monotonously increases(see figures **A–D**). On the other hand, the phase transition of "sergeant" (S_2) is in this regime independent of σ. All graphs from figures **(A–D)** and presented together in figure **(E)**. In the simulation, we used two identical nematogens, which for $w = 0$ exhibit 1st order transition and dimensionless temperatures $T_1^{(c)} = 100$ and $T_2^{(c)} = 105$.

These regions exhibit relatively low and high concentrations of NPs, respectively.

Let us suppose that the mixture remains homogeneous. A simple Maier–Saupe-type analysis (Humphries et al., 1972) presented in Supplementary Appendix SB suggests that in a mixture of two nematogenic components, a free energy density $f^{(coupl)}$ term coupling ordering of both ingredients arises; see the last term in Eq. 1. It should be noted that despite its symmetric structure (e.g., in Eq. 1), the coupling term reads $f^{(coupl)} = -wS_1S_2$); such terms have significantly different impacts on the two components. Here, S_i determines the amplitude of nematic ordering in the ith component. Furthermore, in real samples, different structures of coupling terms arise depending on the type of NPs and their surface treatment. Figure 2 illustrates the "sergeant–soldier" type of behavior, where we consider the simplest possible term (Holbl et al., 2022),

$$f^{(coupl)} = -wS_1^2S_2^2, \tag{4}$$

which does not affect the qualitative order-disorder behavior of individual components. For simplicity, we assume that both components have identical condensation material constants with the exceptions of bulk phase transition temperatures of isolated components and $w > 0$ (i.e., this term tends to increase the degree of order in both components). We assume that an isolated ith component exhibits an isotropic-nematic phase transition at $T_i^{(c)}$, where $T_2^{(c)} > T_1^{(c)}$. Thus, the coupling term is absent in the regime $T > T_2^{(c)}$, where both order parameters are melted. However, in the temperature regime $T < T_2^{(c)}$, the second component condensates. For this reason, the first mesogen experiences the effective free energy density ordering field contribution

$$f^{(coupl)} = -w_{eff}S_1^2, \tag{5}$$

where $w_{eff} = wS_2^2 > 0$. This term renormalizes the phase transition of the first component. It holds

$$T_{eff}^{(c)} = T_1^{(c)} + \frac{w_{eff}}{a_1}, \tag{6}$$

where $T_{eff}^{(c)}$ determines the enhanced phase transition of the first component. Therefore, increasing the value of the coupling strength raises the phase transition temperature of the first component, while the phase transition of the second component is unaffected. The resulting temperature behavior of the mixture is shown in Figure 2. It should be noted that in the case of bilinear coupling (see the last term in Eq. 1), the first component also exhibits pre-transitional effects in the temperature interval $T \in [T_{eff}^{(c)}, T_2^{(c)}]$ if the effective coupling strength is below some critical value. If the latter value is exceeded, the degree of order S_1 exhibits gradual (noncritical) increase with decreasing temperature below $T_2^{(c)}$.

Next, we consider a dilute mixture where the second component consists of anisotropic particles. For illustration, we assume that the free energy F consists of LC condensation, LC nematic elastic, and NP–LC interfacial free energy contributions, where details are given in Supplementary Appendix SA. Of our interest is the impact of NPs

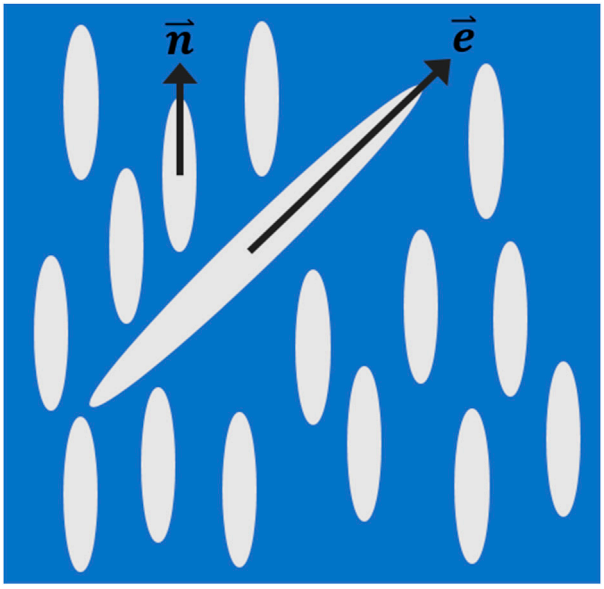

FIGURE 3
Dilute nematic LC—anisotropic NP mixture, where NPs relatively weakly interact with the nematic LC host. Consequently, the nematic LC orientational order, described by the nematic director field $\vec{n}$, is essentially spatially homogeneous. Local anisotropic NP orientation is determined by the unit vector $\vec{e}$.

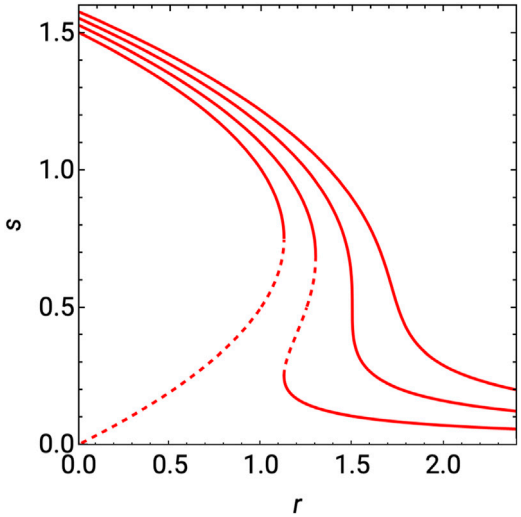

FIGURE 4
Nematic LC order $s = S/S_0$ variations on increasing dimensionless temperature $r = \frac{T-T^*}{T_{IN}-T^*}$ for different values of the effective field σ. The latter arises due to the effective LC–NP coupling. The upper curve corresponds to $\sigma = 0.75$, and the curves below refer to cases $\sigma = 0.5$, $\sigma = 0.25$, and $\sigma = 0$, respectively. In the regime $\sigma < \sigma_c \equiv 0.5$, systems exhibit first-order transition between the isotropic ($\sigma = 0$) or paranematic ($\sigma > 0$) and nematic phase, which takes place at the dimensionless critical temperature $r_c = 1 + \sigma$. The dashed curves describe the degree of nematic order at the free energy density maximum separating paranematic (or isotropic) and nematic (meta) stable states. It should be noted that for $\sigma = 0$ ($\sigma = 0.25$), the global nematic minimum persists in the regime $r < r_c = 1$ ($r < r_c = 1.25$). In the remaining regime, the isotropic (paranematic) phase corresponds to the global minimum.

on the LC order–disorder phase transition. We assume that NPs relatively weakly disrupt the nematic director field, as illustrated in Figure 3. In the nematic phase, $\vec{n}$ is essentially homogeneously aligned along a single symmetry-breaking direction. We assume that a nanoparticle locally enforces orientation along the unit vector $\vec{e}$, which is allowed to fluctuate. We also set S to be essentially spatially homogeneous, i.e., $S \sim \bar{S}$, where $(\bar{\ldots})$ indicates the spatial averaging over the system's volume V. Furthermore, we neglect spatial variations in the nematic director field. With this in mind, it follows (see Supplementary Appendix SA)

$$\frac{F}{V} \sim a_0 (T - T^*) S^2 - bS^3 + cS^4 - p \frac{a_{NP} w S}{v_{NP}} S_2, \tag{7}$$

where $S_2 \equiv \bar{P}_2 = \overline{\frac{(3(\vec{e}\cdot\vec{n})^2 - 1)}{2}}$ measures the orientational order of anisotropic NPs. Quantities N_{NP}, a_{NP}, and v_{NP} stand for the number of NPs, NP's surface area, and NP's volume, respectively. For weakly interacting NPs, it roughly holds (van der Schoot et al., 2008)

$$S_2 \sim \frac{\int P_2 e^{\alpha x} dx}{\int e^{\alpha x} dx}, \tag{8}$$

where $\vec{e} \cdot \vec{n} = x \in [-1, 1]$, $\alpha = a_{NP} w S / (k_B T)$, k_B, and we imposed cylindrical symmetry.

In the limit $\alpha \gg 1$, it holds $S_2 \sim 1$. Eq. 7 yields

$$\tilde{f} \sim r s^2 - 2s^3 + s^4 - \sigma s, \tag{9}$$

where $r = \frac{T-T^*}{T_{IN}-T^*}$ is the reduced temperature, $\tilde{f} = f / (a_0 (T_{IN} - T^*) S_0^2)$, $s = S/S_0$ stands for the scaled nematic order parameter, the scaling unit $S_0 = \frac{b}{2c}$ measures the nematic order at T_{IN} in bulk equilibrium, and $\sigma \sim p \frac{a_{NP} \xi_{IN}^2}{v_{NP} d_e}$ is the effective dimensionless field conjugated to the order parameter. Quantities ξ_{IN} and d_e stand for the nematic correlation length at T_{IN} and the surface extrapolation length (see Eq. (A6)). The latter length describes the effective strength of LC–NP coupling.

The phase behavior of this effective system is as follows. Typical nematic order parameter temperature variations are depicted in Figure 4. For $\sigma < \sigma_c = 0.5$, the system exhibits a first-order transition at $r_c = 1 + \sigma$, where the bulk I–N phase transition corresponds to $r_{IN} = 1$. On the other hand, for $\sigma \geq \sigma_c$, the system exhibits a gradual evolution of nematic order with decreasing temperature.

If $\alpha \sim 1$, the following roughly holds: $S_2 \equiv \bar{P}_2 \sim \frac{a_{NP} w \bar{S}}{k_b T}$. In this case, NPs only renormalize the I–N phase transition temperature. It should be noted that we have neglected the nematic director field distortions in the previously considered estimates.

In the following, we discuss cases where NPs introduce a certain degree of randomness. The I–N phase transition is extremely susceptible to disorder due to the existence of Goldstone modes in the nematic director field in the nematic phase (Kleman and Lavrentovich, 2003; Palffy-Muhoray, 2007). These are the consequences of continuous symmetry breaking, via which bulk nematic equilibrium is established. According to the Imry–Ma theorem (Larkin, 1970; Imry and Ma, 1975), even infinitesimally weak random-field-type disorder is sufficient to break the long-range order (LRO) of the pure bulk phase, which is reached via continuous symmetry breaking. The resulting phase should possess

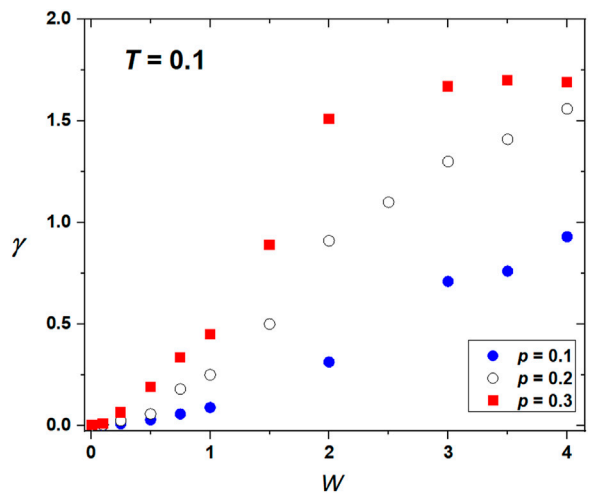

FIGURE 5
Variation of γ on increasing the dimensionless anchoring strength W for different concentrations of NPs, which enforce random-field-like disorder for AH. It should be noted that for $p = 0.1$, one does not achieve SRO, which is anticipated according to the Imry–Ma theorem.

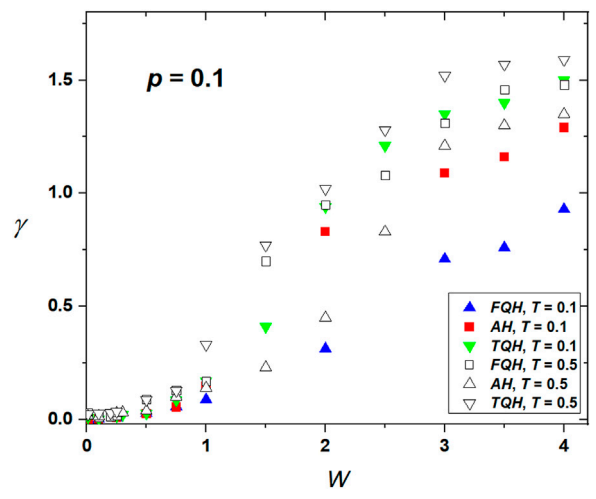

FIGURE 6
Variation of γ on increasing the dimensionless anchoring strength W for different dimensionless temperatures T and histories of samples. For $W > 1$, relatively strong memory effects are observed. Furthermore, in the regime $W < 0.2$, simulations predict LRO.

short-range order (SRO), and the resulting domain-type pattern is predicted to be dominated by a single characteristic domain size $\xi_d \propto w_{RF}^{-\frac{2}{4-d}}$. Here, w_{RF} measures the disorder strength, and d is the space-dimensionality. Therefore, in effectively $d = 2$ or $d = 3$ systems, one expects $\xi_d \propto w_{RF}^{-1}$ and $\xi_d \propto w_{RF}^{-2}$, respectively. However, several later experimental and theoretical systems reveal that the resulting behavior is much more complex. For appropriate conditions, configurations exhibiting quasi-long-range order (QLRO) (Denholm and Sluckin, 1993; Chakrabarti, 1998; Feldman, 2000; Cvetko et al., 2009; Ranjkesh et al., 2014) or even LRO (Chakrabarti, 1998; Bisoyi and Kumar, 2011; Ranjkesh et al., 2014) are reported.

A convenient model to study the impact of NP-imposed randomness on the I–N phase transition is the Lebwohl–Lasher lattice model (Lebwohl and Lasher, 1972). Its key ingredients are presented in Supplementary Appendix SC. Using it, we probe the impact of NP-imposed random-type behavior on the LC order–disorder phase transition in the orientational order. Despite its simplicity, this approach well captures the essential features of LCs. In modeling, we vary the concentration p of sites by imposing a randomly selected orientation with finite disorder strength W. In typical studies focusing on a system's range of orientational order, one commonly measures or calculates the orientational order correlation function $G(r)$. This correlation function measures how orientational correlations decay with relative distance r. However, several studies (Denholm and Sluckin, 1993; Cvetko et al., 2009; Ranjkesh et al., 2014) reveal that $G(r)$ dependence relatively poorly distinguishes between SRO and QLRO. Numerically, it is computationally more effective to extract the range of order using finite-size analysis (Eppenga and Frenkel, 1984; Ranjkesh et al., 2014). Namely, according to the central limit theorem, one expects that $S \equiv \bar{P}_2$ in the case of SRO exhibits scaling behavior

$$\bar{P}_2 \propto L^{-\gamma}, \tag{10}$$

where $\gamma = 3/2$ in $d = 3$. If QLRO replaces SRO, it follows $0 < \gamma < 3/2$. On the other hand, LRO is fingerprinted by $\gamma = 0$.

Our simulations used this finite-scaling approach to determine the range of order on the varying concentration of NPs, their imposed anchoring strength W, and temperature. Furthermore, in the presence of disorder, one expects history-dependent behavior. For this reason, we probed systems' behavior for three different histories, which we refer to as i) annealed history (AH), ii) temperature-quenched history (TQH), and (iii) field-quenched history (FQH). In AH, we gradually decreased temperature stepwise and calculated the structure at a given T by using as the initial "seed" structure the fixed-point configuration calculated at the previous T. In QH, we calculated the structure at a given T by originating from the isotropic phase. Finally, in FQH, the "seed" structure was spatially homogeneously aligned along a single symmetry-breaking direction. In Figures 5, 6, we plot γ for varying several control parameters. In Figure 5, we focus on W-driven behavior for different concentrations of NPs using AH deep in the nematic phase. In Figure 6, we present a more detailed impact of W on LC configurations at one concentration of NPs where we vary the history of samples and probe two different temperatures below the bulk I–N phase transition temperature. One sees that SRO (i.e., configurations characterized by $\gamma = 3/2$ can be reached only for relatively high values of W, especially in diluted samples. The control parameters T and W are given in the dimensionless scaled form. The references are as follows: bulk I–N phase transition is realized at $T \sim 1.1$, and W is measured with respect to LC–LC neighboring molecular interactions. It should be noted that for low enough values of W and p, one observes LRO.

3 Conclusion

We illustrated several mechanisms via which NPs could quantitatively or qualitatively modify the phase behavior of the bulk nematic LC phase. The simplicity of nematic ordering explodes into a rich palette of behaviors enabled by varying control parameters. In the study, we addressed only a few of them: concentration of NPs, nature and strength of NP–LC interactions, and anisotropy of NPs. The diversity of phenomena becomes even wider if the ferromagnetic, ferroelectric, or multiferroic properties of NPs are included. The ferromagnetic nanoparticles dispersed within the liquid crystals provide a new way to develop magneto-optic devices (Ji et al., 2019) that can also be used for THz filtering and modulation, in which sensing applications are becoming increasingly widespread (Abina et al., 2022).

In this paper, we focused only on phase behavior. It should be noted that structural behavior could be even richer. For instance, recent technological advances enable the stabilization of nematic structures incorporating diverse configurations of TDs, i.e., lattices of disclinations (Culbreath et al., 2011; Ackerman et al., 2012a; Ackerman et al., 2012b; Evans et al., 2013; Murray et al., 2014; Glazar et al., 2015; Guo et al., 2016; Peng et al., 2017; Wang et al., 2017; Yu et al., 2019; Sohn et al., 2020; Guo et al., 2021) or other assemblies (Harkai et al., 2020). Such structures could be further modified by appropriate NPs, which could make them more robust or introduce additional functionalities in the system. For example, conductive NPs assembled within a line defect can form a conductive wire (Coursault et al., 2012). Furthermore, recent experiments demonstrated (Harkai et al., 2020) that one could efficiently switch among competing line-defect structures using external fields. If these well-controllable defects would drag trapped NPs with them, one could construct rewritable networks of NPs, which could open doors to diverse applications.

Author contributions

AH, SK, AA, and AZ contributed to the conception and design of the study. AR organized and performed the experimental part. AH wrote the first draft of the manuscript. All authors listed have made a substantial, direct, and intellectual contribution to the work and approved it for publication.

Funding

The authors acknowledge support from the Slovenian Research Agency grants P1-0099, P2-0348, and J1-2457.

Conflict of interest

The authors declare that the research was conducted in the absence of any commercial or financial relationships that could be construed as a potential conflict of interest.

Publisher's note

All claims expressed in this article are solely those of the authors and do not necessarily represent those of their affiliated organizations, or those of the publisher, the editors, and the reviewers. Any product that may be evaluated in this article, or claim that may be made by its manufacturer, is not guaranteed or endorsed by the publisher.

Supplementary material

The Supplementary Material for this article can be found online at: https://www.frontiersin.org/articles/10.3389/frsfm.2023.1193904/full#supplementary-material

References

Abina, A., Puc, U., and Zidanšek, A. (2022). Challenges and opportunities of terahertz technology in construction and demolition waste management. *J. Environ. Manage* 315, 115118. doi:10.1016/j.jenvman.2022.115118

Ackerman, P. J., Qi, Z., Lin, Y., Twombly, C. W., Laviada, M. J., Lansac, Y., et al. (2012). Laser-directed hierarchical assembly of liquid crystal defects and control of optical phase singularities. *Sci. Rep.* 2, 414. doi:10.1038/srep00414

Ackerman, P. J., Qi, Z., and Smalyukh, II. Optical generation of crystalline, quasicrystalline, and arbitrary arrays of torons in confined cholesteric liquid crystals for patterning of optical vortices in laser beams. *Phys. Rev. E.* 2012;86, 021703, doi:10.1103/physreve.86.0217032, 1).

Anderson, V. J., Terentjev, E. M., Meeker, S. P., Crain, J., and Poon, W. C. K. (2001). Cellular solid behaviour of liquid crystal colloids - 1. Phase separation and morphology. *Eur. Phys. J. E* 4 (1), 11–20. doi:10.1007/pl00013680

Balazs, A. C., Emrick, T., and Russell, T. P. (1979). Nanoparticle polymer composites: Where two small worlds meet. *Science* 314 (5802), 1107–1110. doi:10.1126/science.1130557

Bellini, T., Buscaglia, M., Chiccoli, C., Mantegazza, F., Pasini, P., and Zannoni, C. (2002). Nematics with quenched disorder: How long will it take to heal? *Phys. Rev. Lett.* 88 (24), 245506. doi:10.1103/physrevlett.88.245506

Bellini, T., Buscaglia, M., Chiccoli, C., Mantegazza, F., Pasini, P., and Zannoni, C. (2000). Nematics with quenched disorder: What is left when long range order is disrupted? *Phys. Rev. Lett.* 85 (5), 1008–1011. doi:10.1103/physrevlett.85.1008

Bisoyi, H. K., and Kumar, S. (2011). Liquid-crystal nanoscience: An emerging avenue of soft self-assembly. *Chem. Soc. Rev.* 40 (1), 306–319. doi:10.1039/b901793n

Bury, P., Vevericik, M., Cernobila, F., Tomasovicova, N., Zakut'anska, K., Kopcansky, P., et al. (2022). Role of magnetic nanoparticles size and concentration on structural changes and corresponding magneto-optical behavior of nematic liquid crystals. *Nanomaterials* 12 (14), 2463. doi:10.3390/nano12142463

Buscaglia, M., Bellini, T., Chiccoli, C., Mantegazza, F., Pasini, P., Rotunno, M., et al. Memory effects in nematics with quenched disorder. *Phys. Rev. E.* 2006;74, 011706, doi:10.1103/physreve.74.0117061, 1).

Chakrabarti, J. (1998). Simulation evidence of critical behavior of isotropic-nematic phase transition in a porous medium. *Phys. Rev. Lett.* 81 (2), 385–388. doi:10.1103/physrevlett.81.385

Cleaver, D. J., Kralj, S., Sluckin, T. J., and Allen, M. P. (1996). "The random anisotropy nematic spin model," in *Liquid crystals in complex geometries: Formed by polymer and porous networks* G. P. Crawford and S. Žumer (Oxford: Oxford University Press).

Cordoyiannis, G., Kralj, S., Nounesis, G., Zumer, S., and Kutnjak, Z., Soft-stiff regime crossover for an aerosil network dispersed in liquid crystals. *Phys. Rev. E.* 2006;73, 031707, doi:10.1103/physreve.73.0317073, 1).

Coursault, D., Grand, J., Zappone, B., Ayeb, H., Levi, G., Felidj, N., et al. (2012). Linear self-assembly of nanoparticles within liquid crystal defect arrays. *Adv. Mater.* 24 (11), 1461–1465. doi:10.1002/adma.201103791

Crawford, G. P., and Žumer, S. (1996). *Liquid crystals in complex geometries formed by polymer and porous networks.* London: Taylor & Francis.

Culbreath, C., Glazar, N., and Yokoyama, H. (2011). Note: Automated maskless micro-multidomain photoalignment. *Rev. Sci. Instrum.* 82 (12), 126107. doi:10.1063/1.3669528

Cvetko, M., Ambrožič, M., and Kralj, S. (2009). Memory effects in randomly perturbed systems exhibiting continuous symmetry breaking. *Liq. Cryst.* 36 (1), 33–41. doi:10.1080/02678290802638431

de Gennes, P. G. (1995). *The physics of liquid crystals*. Oxford: Oxford University Press.

Denholm, D. R., and Sluckin, T. J. (1993). Monte Carlo studies of two-dimensional random-anisotropy magnets. *Phys. Rev. B* 48 (2), 901–912. doi:10.1103/physrevb.48.901

Doi, M. (1981). Molecular-Dynamics and rheological properties of concentrated-solutions of rodlike polymers in isotropic and liquid-crystalline phases. *J. Polym. Sci. PART B-POLYMER Phys.* 19 (2), 229–243. doi:10.1002/pol.1981.180190205

Drozd-Rzoska, A., Starzonek, S., Rzoska Sylwester, J., and Kralj, S. (2019). Nanoparticle-controlled glassy dynamics in nematogen-based nanocolloids. *Phys. Rev. E* 99 (5), 052703. doi:10.1103/physreve.99.052703

Emdadi, M., Poursamad, J. B., Sahrai, M., and Moghadas, F. (2018). Investigation of nematic liquid crystals doped with spherical multiferroic nanoparticles in the presence of a magnetic field. *Braz. J. Phys.* 48 (5), 433–441. doi:10.1007/s13538-018-0590-8

Emdadi, M., Poursamad, J. B., Sahrai, M., and Moghaddas, F. (2018). Behaviour of nematic liquid crystals doped with ferroelectric nanoparticles in the presence of an electric field. *Mol. Phys.* 116 (12), 1650–1658. doi:10.1080/00268976.2018.1441462

Eppenga, R., and Frenkel, D. (1984). Monte-carlo study of the isotropic and nematic phases of infinitely thin hard platelets. *Mol. Phys.* 52 (6), 1303–1334. doi:10.1080/00268978400101951

Evans, J. S., Ackerman, P. J., Broer, D. J., van de Lagemaat, J., and Smalyukh, II (2013). Optical generation, templating, and polymerization of three-dimensional arrays of liquid-crystal defects decorated by plasmonic nanoparticles. *Phys. Rev. E* 87 (3), 032503. doi:10.1103/physreve.87.032503

Feldman, D. E. (2000). Quasi-long-range order in nematics confined in random porous media. *Phys. Rev. Lett.* 84 (21), 4886–4889. doi:10.1103/physrevlett.84.4886

Flory, P. J. (1956). Phase equilibria in solutions of rod-like particles. *Proc. R. Soc. Lond A* 234, 73–89.

Glazar, N., Culbreath, C., Li, Y., and Yokoyama, H. (2015). Switchable liquid-crystal phase-shift mask for super-resolution photolithography based on Pancharatnam-Berry phase. *Appl. Phys. EXPRESS* 8 (11), 116501. doi:10.7567/apex.8.116501

Guo, Y., Jiang, M., Afghah, S., Peng, C., Selinger, R. L. B., Lavrentovich, O. D., et al. (2021). Photopatterned designer disclination networks in nematic liquid crystals. *Adv. Opt. Mater* 9 (16), 2100181. doi:10.1002/adom.202100181

Guo, Y., Jiang, M., Peng, C., Sun, K., Yaroshchuk, O., Lavrentovich, O., et al. (2016). High-Resolution and high-throughput plasmonic photopatterning of complex molecular orientations in liquid crystals. *Adv. Mater.* 28 (12), 2353–2358. doi:10.1002/adma.201506002

Hamley, I. W. (2003). Nanotechnology with soft materials. *Angew. Chemie-International Ed.* 42 (15), 1692–1712. doi:10.1002/anie.200200546

Harkai, S., Murray, B. S., Rosenblatt, C., and Kralj, S. (2020). Electric field driven reconfigurable multistable topological defect patterns. *Phys. Rev. Res.* 2 (1), 013176. doi:10.1103/physrevresearch.2.013176

Harris, R., Plischke, M., and Zuckermann, M. J. (1973). New model for amorphous magnetism. *Phys. Rev. Lett.*31 (3), 160–162. doi:10.1103/physrevlett.31.160

Hegmann, T., Qi, H., and Marx, V. M. (2007). Nanoparticles in liquid crystals: Synthesis, self-assembly, defect formation and potential applications. *J. Inorg. Organomet. Polym. Mater* 17 (3), 483–508. doi:10.1007/s10904-007-9140-5

Holbl, A., Pal, K., Slavinec, M., and Kralj, S. (2022). Slave-master mechanism of thermotropic liquid crystal phase transitional behavior. *Phys. B-CONDENSED MATTER* 642, 414142. doi:10.1016/j.physb.2022.414142

Humphries, R. L., James, P. G., and Luckhurst, G. R. (1972). Molecular field treatment of nematic liquid-crystals. *J. Chem. Society-Faraday Trans. II* 68 (6), 1031. doi:10.1039/f29726801031

Imry, Y., and Ma, S. (1975). Random-field instability of the ordered state of continuous symmetry. *Phys. Rev. Lett.* 35 (21), 1399–1401. doi:10.1103/physrevlett.35.1399

Jahanbakhsh, F., Poursamad, J. B., Ara, M. H. M., Lorenz, A., Khoshsima, H., and Darabi, M. (2019). Dispersion of multiferroic BiFeO3 nanoparticles in nematic liquid crystals. *Appl. Phys. A-Materials Sci. Process.* 125 (12), 877. doi:10.1007/s00339-019-3153-0

Ji, Y., Fan, F., Xu, S., Yu, J., and Chang, S. (2019). Manipulation enhancement of terahertz liquid crystal phase shifter magnetically induced by ferromagnetic nanoparticles. *Nanoscale* 11 (11), 4933–4941. doi:10.1039/c8nr09259a

Jin, T., and Finotello, D. (2001). Aerosil dispersed in a liquid crystal: Magnetic order and random silica disorder. *Phys. Rev. Lett.* 86 (5), 818–821. doi:10.1103/physrevlett.86.818

Karatairi, E., Rozic, B., Kutnjak, Z., Tzitzios, V., Nounesis, G., Cordoyiannis, G., et al. Nanoparticle-induced widening of the temperature range of liquid-crystalline blue phases. *Phys. Rev. E.* 2010;81, 041703, doi:10.1103/physreve.81.0417034, 1).

Kikuchi, H., Yokota, M., Hisakado, Y., Yang, H., and Kajiyama, T. (2002). Polymer-stabilized liquid crystal blue phases. *Nat. Mater* 1 (1), 64–68. doi:10.1038/nmat712

Kleman, M., and Lavrentovich, O. D. (2003). *Soft matter physics: An introduction*. New York: Springer Science & Business Media.

Kralj, S., and Virga, E. G. (2001). Universal fine structure of nematic hedgehogs. *J. Phys. A Math. Gen.* 34 (4), 829–838. doi:10.1088/0305-4470/34/4/309

Kumar, S. (2014). Discotic liquid crystal-nanoparticle hybrid systems. *NPG Asia Mater* 6, e82. doi:10.1038/am.2013.75

Kurik, M. V., and Lavrentovich, O. D. (1988). Defects in liquid-crystals - homotopy-theory and experimental investigations. *Uspekhi Fiz. Nauk.* 154 (3), 381–431. doi:10.3367/ufnr.0154.198803b.0381

Kyrou, C., Kralj, S., Panagopoulou, M., Raptis, Y., Nounesis, G., and Lelidis, I. (2018). Impact of spherical nanoparticles on nematic order parameters. *Phys. Rev. E* 97 (4), 042701. doi:10.1103/physreve.97.042701

Kyrou, C., Tsiourvas, D., Kralj, S., and Lelidis, I. (2020). Effect of superhydrophobic nanoplatelets on the phase behaviour of liquid crystals. *J. Mol. Liq.* 298, 111984. doi:10.1016/j.molliq.2019.111984

Lagerwall, J. P., and Scalia, G. (2017). "Liquid crystals with nano and microparticles," in *2 volumes) (series in soft condensed matter book 7)* (Florida: CRC Press).

Lagerwall, J. P. F., and Scalia, G. (2012). A new era for liquid crystal research: Applications of liquid crystals in soft matter nano-bio- and microtechnology. *Curr. Appl. Phys.* 12 (6), 1387–1412. doi:10.1016/j.cap.2012.03.019

Lahiri, T., Pushkar, S. K., and Poddar, P. (2020). Theoretical study on the effect of electric field for carbon nanotubes dispersed in nematic liquid crystal. *Phys. B-Condensed Matter* 588, 412177. doi:10.1016/j.physb.2020.412177

Larkin, A. I. (1970). Effect of inhomogeneities on structure of mixed state of superconductors. *Sov. Phys. JETP-USSR* 31 (4), 784.

Lavrentovich, O. D. (1998). Topological defects in dispersed words and worlds around liquid crystals, or liquid crystal drops. *Liq. Cryst.* 24 (1), 117–126. doi:10.1080/026782998207640

Lavric, M., Cordoyiannis, G., Kralj, S., Tzitzios, V., Nounesis, G., and Kutnjak, Z. (2013). Effect of anisotropic MoS2 nanoparticles on the blue phase range of a chiral liquid crystal. *Appl. Opt.* 52 (22), E47–E52. doi:10.1364/ao.52.000e47

Lavric, M., Tzitzios, V., Kralj, S., Cordoyiannis, G., Lelidis, I., Nounesis, G., et al. (2013). The effect of graphene on liquid-crystalline blue phases. *Appl. Phys. Lett.* 103 (14), 143116. doi:10.1063/1.4824424

Lebwohl, P. A., and Lasher, G. (1972). Nematic-liquid-Crystal order—a Monte Carlo calculation. *Phys. Rev. A Coll. Park)* 6 (1), 426–429. doi:10.1103/physreva.6.426

Lelidis, I., Nobili, M., and Durand, G. (1993). Electric-field-Induced change of the order-parameter in a nematic liquid-crystal. *Phys. Rev. E* 48 (5), 3818–3821. doi:10.1103/physreve.48.3818

Leon, N., Korb, J. P., Bonalde, I., and Levitz, P. (2004). Universal nuclear spin relaxation and long-range order in nematics strongly confined in mass fractal silica gels. *Phys. Rev. Lett.* 92 (19), 195504. doi:10.1103/physrevlett.92.195504

Li, F., Buchnev, O., Il Cheon, C., Glushchenko, A., Reshetnyak, V., Reznikov, Y., et al. (2006). Orientational coupling amplification in ferroelectric nematic colloids. *Phys. Rev. Lett.* 97 (14), 147801. doi:10.1103/physrevlett.97.147801

Liu, F., Ma, G., and Zhao, D. (2018). Nickel nanoparticle-stabilized room-temperature blue-phase liquid crystals. *Nanotechnology* 29 (28), 285703. doi:10.1088/1361-6528/aabaa4

Liu, Q., Cui, Y., Gardner, D., Li, X., He, S., and Smalyukh, II (2010). Self-alignment of plasmonic gold nanorods in reconfigurable anisotropic fluids for tunable bulk metamaterial applications. *Nano Lett.* 10 (4), 1347–1353. doi:10.1021/nl9042104

Ma, Z., Gao, Y., and Cao, H. (2022). The effect of chemically modified multi-walled carbon nanotubes on the electro-optical properties of a twisted nematic liquid crystal display mode. *Cryst. (Basel)* 12 (10), 1482. doi:10.3390/cryst12101482

Mermin, N. D. (1979). The topological theory of defects in ordered media. *Rev. Mod. Phys.* 51 (3), 591–648. doi:10.1103/revmodphys.51.591

Mertelj, A., Lisjak, D., Drofenik, M., and Copic, M. (2013). Ferromagnetism in suspensions of magnetic platelets in liquid crystal. *Nature* 504 (7479), 237–241. doi:10.1038/nature12863

Moghadas, F., Khoshsima, H., and Olyaeefar, B. (2015). High diffraction efficiency in permanent optical memories based on Methyl Red doped liquid crystal. *Opt. Quantum Electron* 47 (2), 225–233. doi:10.1007/s11082-014-9906-2

Murray, B. S., Pelcovits, R. A., and Rosenblatt, C. (2014). Creating arbitrary arrays of two-dimensional topological defects. *Phys. Rev. E* 90 (5), 052501. doi:10.1103/physreve.90.052501

Nobili, D., and Durand, G. (1992). Disorientation-induced disordering at a nematic-liquid-crystal-solid interface. *Phys. Rev. A* 46 (10), R6174–R6177. doi:10.1103/physreva.46.r6174

Onsager, L. (1949). The effects of shape on the interaction of colloidal particles. *Ann. N. Y. Acad. Sci.* 51 (4), 627–659. Available from:. doi:10.1111/j.1749-6632.1949.tb27296.x

Oswald, P., and Pieranski, P. (2019). *Nematic and cholesteric liquid crystals concepts and physical properties illustrated by experiments*. Florida: CRC Press.

Palffy-Muhoray, P. (2007). The diverse world of liquid crystals. *Phys. Today* 60 (9), 54–60. doi:10.1063/1.2784685

Peng, C., Guo, Y., Turiv, T., Jiang, M., Wei, Q. H., and Lavrentovich, O. D. (2017). Patterning of lyotropic chromonic liquid crystals by photoalignment with photonic metamasks. *Adv. Mater.* 29 (21), 1606112. doi:10.1002/adma.201606112

Pires, D., Fleury, J. B., and Galerne, Y. (2007). Colloid particles in the interaction field of a disclination line in a nematic phase. *Phys. Rev. Lett.* 98 (24), 247801. doi:10.1103/physrevlett.98.247801

Popa-Nita, V., and Kralj, S. (2006). Random anisotropy nematic model: Nematic-non-nematic mixture. *Phys. Rev. E Stat. Nonlin Soft Matter Phys.* 73 (4), 041705–041708. doi:10.1103/physreve.73.041705

Poulin, P., Stark, H., Lubensky, T. C., and Weitz, D. A. (1979). Novel colloidal interactions in anisotropic fluids. *Science* 275 (5307), 1770–1773. doi:10.1126/science.275.5307.1770

Poursamad, J. B., and Emdadi, M. (2019). Optical nonlinearity of liquid crystals in the presence of chained ferroelectric nanoparticles. *Acta Phys. Pol. A* 136 (6), 861–865. doi:10.12693/aphyspola.136.861

Poursamad, J. B., and Hallaji, T. (2017). Freedericksz transition in smectic-A liquid crystals doped by ferroelectric nanoparticles. *Phys. B-Condensed Matter* 504, 112–115. doi:10.1016/j.physb.2016.10.022

Radzihovsky, L., and Toner, J. (1997). Nematic-to-smectic-A transition in aerogel. *Phys. Rev. Lett.* 79 (21), 4214–4217. doi:10.1103/physrevlett.79.4214

Ranjkesh, A., Ambrozic, M., Kralj, S., and Sluckin, T. J. (2014). Computational studies of history dependence in nematic liquid crystals in random environments. *Phys. Rev. E* 89 (2), 022504. doi:10.1103/physreve.89.022504

Relaix, S., Leheny, R. L., Reven, L., and Sutton, M., Memory effect in composites of liquid crystal and silica aerosil. *Phys. Rev. E.* 2011;84, 061705, doi:10.1103/physreve.84.061705

Rotunno, M., Buscaglia, M., Chiccoli, C., Mantegazza, F., Pasini, P., Bellini, T., et al. (2005). Nematics with quenched disorder: Pinning out the origin of memory. *Phys. Rev. Lett.* 94 (9), 097802. doi:10.1103/physrevlett.94.097802

Rozic, B., Tzitzios, V., Karatairi, E., Tkalec, U., Nounesis, G., Kutnjak, Z., et al. (2011). Theoretical and experimental study of the nanoparticle-driven blue phase stabilisation. *Eur. Phys. J. E* 34 (2), 17. doi:10.1140/epje/i2011-11017-8

Schopohl, N., and Sluckin, T. J. (1987). Defect core structure in nematic liquid-crystals. *Phys. Rev. Lett.* 59 (22), 2582–2584. doi:10.1103/physrevlett.59.2582

Skarabot, M., Mottram, N. J., Kaur, S., Imrie, C. T., Forsyth, E., Storey, J. M. D., et al. (2022). Flexoelectric polarization in a nematic liquid crystal enhanced by dopants with different molecular shape polarities. *ACS Omega* 7 (11), 9785–9795. doi:10.1021/acsomega.2c00023

Skarabot, M., Ryzhkova, A. V., and Musevic, I. (2018). Interactions of single nanoparticles in nematic liquid crystal. *J. Mol. Liq.* 267, 384–389. doi:10.1016/j.molliq.2018.01.068

Sohn, H. R. O., Liu, C. D., Voinescu, R., Chen, Z., and Smalyukh, II (2020). Optically enriched and guided dynamics of active skyrmions. *Opt. Express* 28 (5), 6306–6319. doi:10.1364/oe.382845

Sumandra, S. B., Mahendra, B., Nugroho, F., and Yusuf, Y. (2022). Alignment of carbon nanotubes under the influences of nematic liquid crystals and electric fields - an analytical study. *Int. J. Comput. Mater Sci. Eng.* 11 (02). doi:10.1142/s2047684121500330

van der Schoot, P., Popa-Nita, V., and Kralj, S. (2008). Alignment of carbon nanotubes in nematic liquid crystals. *J. Phys. Chem. B* 112 (15), 4512–4518. doi:10.1021/jp712173n

Wang, L., He, W., Xiao, X., Meng, F., Zhang, Y., Yang, P., et al. (2012). Hysteresis-free blue phase liquid-crystal-stabilized by ZnS nanoparticles. *Small* 8 (14), 2189–2193. doi:10.1002/smll.201200052

Wang, M., Li, Y., and Yokoyama, H. (2017). Artificial web of disclination lines in nematic liquid crystals. *Nat. Commun.* 8, 388. doi:10.1038/s41467-017-00548-x

Yoshida, H., Tanaka, Y., Kawamoto, K., Kubo, H., Tsuda, T., Fujii, A., et al. (2009). Nanoparticle-stabilized cholesteric blue phases. *Appl. Phys. EXPRESS* 2 (12), 121501. doi:10.1143/apex.2.121501

Yu, H., Jiang, M., Guo, Y., Turiv, T., Lu, W., Ray, V., et al. (2019). Plasmonic metasurfaces with high UV-vis transmittance for photopatterning of designer molecular orientations. *Adv. Opt. Mater* 7 (11), 1900117. doi:10.1002/adom.201900117